RECENT DEVELOPMENTS IN THE ISTTOK HEAVY ION BEAM DIAGNOSTIC

I.S. Nedzelskiy, A. Malaquias, R.B. Henriques, R. Sharma

Instituto de Plasmas e Fusão Nuclear, Instituto Superior Técnico, Universidade de Lisboa, Lisboa, Portugal

E-mail: igorz@ipfn.ist.utl.pt

The heavy ion beam diagnostic (HIBD) presents a powerful tool for investigations of hot plasmas in thermonuclear devices with magnetic confinement. When injected into the plasma, the primary probing beam of singly charged positive ions is ionized to a doubly charged state by impact with the plasma electrons and separated from the primaries due to the confining magnetic field of the plasma device. The resulting secondary ions are collected outside the plasma. The plasma parameters that can be measured by the HIBD are: the plasma electron density and temperature, and the electric and magnetic potentials. On the small tokamak ISTTOK (R = 0.46 m, a = 0.085 m, B = 0.5 T, I_p = 4…6 kA, $<n_e>$ = 5 × 10^{18} m^{-3}, T_e = 120 eV), the HIBD is based on a 20 keV Xe^+ (or Cs^+) beam injector and a multiple cell array detector (MCAD) collecting a fan of secondary Xe^{2+} (or Cs^{2+}) ions emerging from the plasma along the primary beam trajectory. This paper describes the recent developments and improvements in the ISTTOK HIBD secondary beam detection. The capabilities of new detection system are illustrated by recent results of ISTTOK plasma MHD activity and electrode biasing studies. The on going developments of the multichannel multi-slit 90° cylindrical energy analyzer for the plasma potential and its fluctuations measurements and a novel approach of the HIBD use in real-time vertical plasma position control are also considered.

PACS: 52.55.Fa, 52.70.-m

INTRODUCTION

The heavy ion beam diagnostic (HIBD) has been a subject of study in fusion plasma diagnostics for about fifty years since the pioneering work of the HIBD inventors F. Jobes and R. Hickok on the ST tokamak [1]. The HIBP principle is rather simple and explained by Fig. 1.

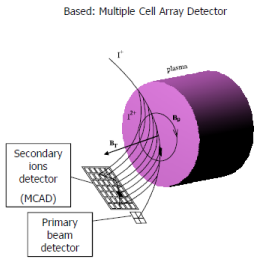

Fig. 1. HIBD principle

A beam of single charged ions (primary ions) is injected into the plasma across the confined magnetic field. The ions of double charge state (secondary ions) are created in collisions with plasma electrons and, after separation from the primary beam due to magnetic field, are collected outside the plasma. For a fixed single point detector the position of ionization point (sample volume) can be effectively moved with changing of beam injection angle and/or energy. Alternatively, the fan of secondary ions emerging from primary beam along the fixed trajectory crossing the plasma can be collected by a multiple cell detector. In such detection scheme a number of sample volumes are recorded simultaneously which is essential in investigation of the plasma parameters fluctuations.

The intensity of the secondary beam relates to the plasma parameters as:

$$I_s = 2I_p F_{pl} F_{s1} \sigma_{eff}(T_e) l_{sv} n_e(r_{sv}),$$

where I_p is the intensity of the primary beam, F_{pl} and F_{s1} are the primary and secondary beam exponential attenuation factors, $\sigma_{eff}(T_e)$ is the effective ionization cross-section (function of the plasma electron temperature), l_{sv} is the sample volume dimension, and $n_e(r_{sv})$ is the average over the sample volume plasma electron density. This relation is the basis for the plasma electron density and temperature measurements. On the other hand, the energy of the secondary ion at the ionization point is changed exactly as the local plasma potential value, thus allowing for the measurements of that important plasma parameter. Also, the HIBP capability to retrieve plasma current profile from the measurements of secondary beam shift due to the plasma current magnetic field should be mentioned.

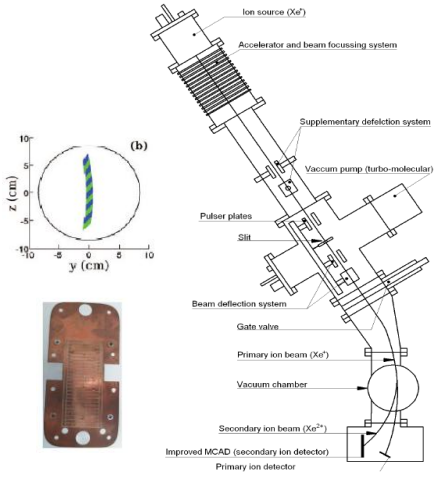

Fig. 2. Schematic of HIBD on the tokamak ISTTOK

The HIBD on the small tokamak ISTTOK (R = 0.46 m, a = 0.085 m, B = 0.5 T, I_p = 4-6 kA, $\langle n_e \rangle = 5 \times 10^{18}$ m^{-3}, T_e = 120 eV) is based on the 20 keV Xe^+ (or Cs^+) beam injector (operating with plasma ion source [2]) and a multiple cell array detector (MCAD) collecting a fan of secondary Xe^{2+} (or Cs^{2+}) ions emerging from the plasma along the primary beam trajectory as sketched in Fig. 2. The MCAD (the picture also shown in Fig. 2) basically presents a flat matrix of a number of collector cells [3]. With such very simple MCAD, the profiles of plasma electron density and temperature were measured in early experiments with HIBD on the ISTTOK [4]. Also, the plasma current profile evolution was obtained from the measurements of toroidal shifts of the secondary ions [5].

1. RECENT DEVELOPMENTS AND ILLUSTRATIVE RESULTS

When studying the turbulent characteristic of the plasma, a high gain, wide bandwidth and low noise detectors and amplifiers are required. Recent developments and improvements of the ISTTOK HIBD secondary beam detection allow for the increase of the detector signal-to-noise ratio and amplifiers bandwidth, thus improving the overall performance of the HIBD operation and quality of the obtained data.

1.1. MCAD AND ELECTRONICS

Measurements with MCAD are efficient in a close to the plasma arrangement of the detector, operating therefore in strong radiation environment (mainly UV), that can result in spurious background signal from the cells due to electron emission effect.

To achieve an effective shielding from emitted electrons, in the new MCAD design the cells are not flat, but consist of two similar geometry Γ/L-like shaped copper plates combined together as shown in Fig. 3.

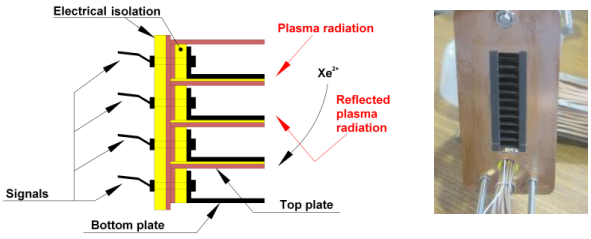

Fig. 3. Sketch and picture of new MCAD

In such configuration, the cell presents an effectively Faraday cup-like structure 10 mm of deepness. 12 cells are individually attached in a column stack fixed on insulator plate and then painted by colloidal graphite to reduce the electron emission yield. The stack is shielded by a copper plate baffle arrangement with opening face (12×60 mm) to the plasma. In this new version of the MCAD the bottom L-plates of the cells are opened for the secondary ions and plasma radiation. Contrary, the top Γ-plates of the cells are almost completely shielded from the secondary ions and can be biased to suppress the secondary electrons and photo-electrons created on the bottom plates. Fig. 4 illustrates the efficiency of the modified MCAD on an example of the square-wave chopped secondary ions signal obtained on one MCAD cell in two plasma shots without and with cell biasing at -3 V.

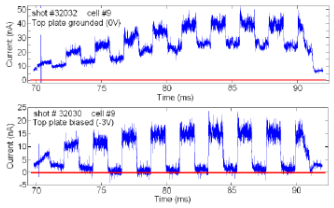

Fig. 4. Signal from one cell without and with biasing

Complete suppression of the plasma background signal is achieved.

The HIBD signal conditioning system has been improved with elaborated small size and low cost transimpedance two stages amplifiers with gain of 2×10^7 V/A, 0.5 nA, rms of noise and 400 kHz bandwidth. The whole amplification system consists of up to 50 amplifier modules connected side by side in several layers, Fig. 5,a. One side is connected directly to the tokamak diagnostic port flange with two D25 connectors. The amplification system is powered by batteries and shielded with Mu-metal box to reduce the electromagnetic induced noise, Fig. 5,b. Signals, coming from the amplifiers, are digitized at 2 MHz sampling rate and stored by the ISTTOK data acquisition system.

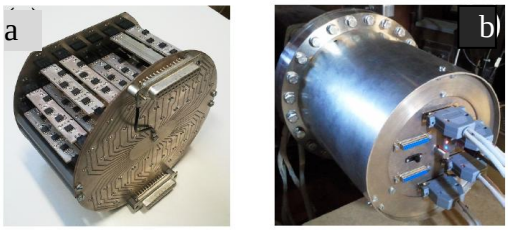

Fig. 5. Pictures of amplification system

The improved detection system results in 3 time increase of the signal-to-noise ratio.

1.2. STUDY OF MHD ACTIVITY [7]

The results presented in this subsection have been obtained in the ISTTOK discharges with B_T = 0.45 T, I_p = 6 kA, and $\langle n_e \rangle = 4 \times 10^{18}$ m^{-3}, characterized by repetitive bursts of MHD activity and density drops. It should be noted that the core electron temperature in the ISTTOK is not high, ~120 eV, meaning that the HIBD signal amplitude and profile is not only determined by the plasma electron density value and profile, but also by the value and profile of the electron temperature (via $\sigma_{1,2}(T_e)$). Therefore, for ISTTOK plasmas it is more correct to speak about measurements of the $n_e\sigma_{1,2}(T_e)$ product profile, which may be considered as a proxy of the plasma pressure.

Fig. 6 shows the combined view of the $n_e\sigma_{1,2}(T_e)$ profile, the signals from the Mirnov coil, and the line integrated density during the MHD event. The Mirnov coil signal indicates a violent and unstable growing

before the crash. The $n_e\sigma_{1,2}(T_e)$ profile starts to fluctuate mainly in the plasma core with growing amplitude up to 30 % of the absolute value, correlating with the MHD fluctuations. After the crash (from 113.08 ms) the MHD activity and fluctuations in the $n_e\sigma_{1,2}(T_e)$ profile are significantly reduced and the plasma remains in a "quiescent" state during some time.

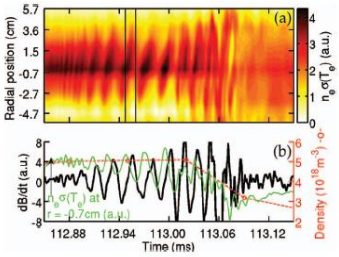

Fig. 6. $n_e\sigma_{1,2}(T_e)$ profile, Mirnov coil signal, and the line integrated density during the MHD event

Fig. 7 presents a detail view of $n_e\sigma_{1,2}(T_e)$ radial profile during the MHD event (112.8…113.2 ms) indicating the transition from a peaked to flat profile. However, the integrated value of $n_e\sigma_{1,2}(T_e)$ remains the same (<2% of variation) before and after the crash, while the line integrated density signal drops on 40% (as measured by interferometer). The observed property can be due to above mentioned combined response of the $n_e\sigma_{1,2}(T_e)$ product on variations in n_e and T_e.

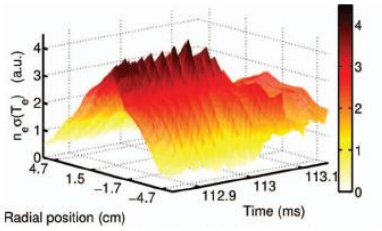

Fig. 7. $n_e\sigma_{1,2}(T_e)$ radial profile during MHD event

As the effective detector line of ISTTOK HIBD intersects plasma almost by strait line crossing the plasma axis (see Fig. 1), it presents an interest to search and identify a tearing mode (TM) structure by the phase reversal of the respective fluctuations between two neighboring cells.

Such a signature have been observed in the ISTTOK discharge with slow ramp-up plasma current (4…7 kA in 18 ms) as shown in Fig. 8 for filtered HIBD signals at the dominant MHD frequency (50…70 kHz) of m=4 mode.

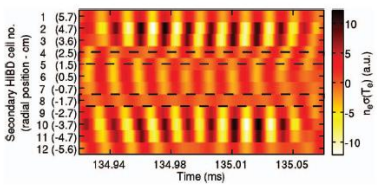

Fig. 8. Signals from MCAD cells

A clear phase reversal between two successive cells (marked by dashed lines) is observed, indicating the rational flux surface location at $r \sim \pm 2$ cm.

1.3. ELECTRODE BIASING EXPERIMENTS

Edge plasma biasing experiments have been performed on many tokamaks demonstrating a clear correlation between the $E\times B$ flow shear velocity and turbulence control [8]. In ISTTOK, the plasma fluctuations can be measured in the whole minor radius using the HIBD (core and inner edge) and LPs (edge) diagnostics together, that present a special interest as the link between plasma core and edge can be studied. Typically, to maximize the improvement in confinement, a movable graphite electrode is located 2…2.5 cm inside the last closed flux surface and biased at +80 V. Improved confinement regimes in ISTTOK are characterized by an averaged plasma density $<n_e>$ increase, H_α radiation decrease, edge turbulent transport decrease as shown in Fig. 9.

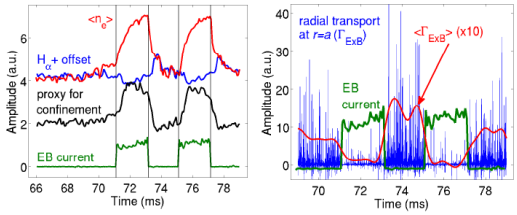

Fig. 9. $<n_e>$, H_α, EB current, ETT during biasing

Fig. 10 presents the $n_e\sigma_{eff}(T_e)$ and ion saturation current I_{sat} profiles during normal and improved confinement phases. During EB, the $n_e\sigma_{eff}(T_e)$ profile is peaked, while I_{sat} flattened.

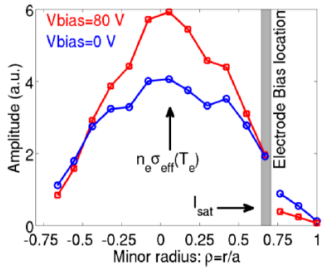

Fig. 10. $n_e\sigma_{eff}(T_e)$ and I_{sat} profiles during biasing

The evolution of the turbulent transport and the $n_e\sigma_{eff}(T_e)$ profile during a full EB cycle is shown in Fig. 11. Just after EB transitions (solid vertical lines) the transport is modified within the turbulence characteristic time of ~10 μs. The $n_e\sigma_{eff}(T_e)$ profile major changes, indicated by the dashed lines in Fig. 11, only happen after ~150 μs, corresponding to the particle confinement time. It is also observed that the $n_e\sigma_{eff}(T_e)$ profile reaches its maximum about 1ms after the EB is applied.

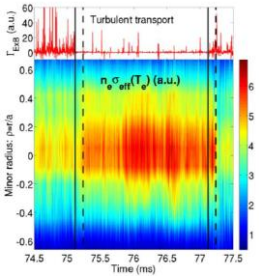

Fig. 11. Turbulent transport and the $n_e\sigma_{eff}(T_e)$ profile during EB

During non EB, HIBD peripheral signals are usually dominated by MHD activity fluctuations (confirmed by Mirnov coils signal). When EB is applied, the MHD activity strongly decreases on both peripheral HIBD channels and Mirnov coils as illustrated in Fig. 12. It is also observed an increase of fluctuations in the central HIBD channels the nature of which is a matter for future research.

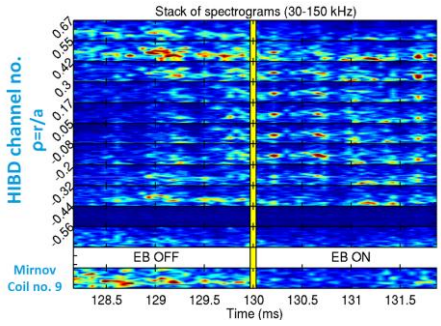

Fig. 12. Spectrogram of MCAD and one MC signals during EB

2. ON GOING DEVELOPMENTS

2.1. 90° CYLINDRICAL ENERGY ANALYZER

In order to extend the capabilities of MCAD to measure the plasma potential and its fluctuations in the $\Delta E/E < 10^{-3}$ range, a multiple-channel multi-slit 90° cylindrical energy analyzer (CEA) has been proposed, Fig. 13. The main advantage of the considered 90° CEA is compactness to suit the geometric constraints of experimental conditions on ISTTOK.

The SIMION code has been applied to minimize the angular aberration and to increase the energy resolution beyond the ideal, implementing an approach to take advantage of the strong lensing properties of fringing fields [9] and deceleration inside CEA.

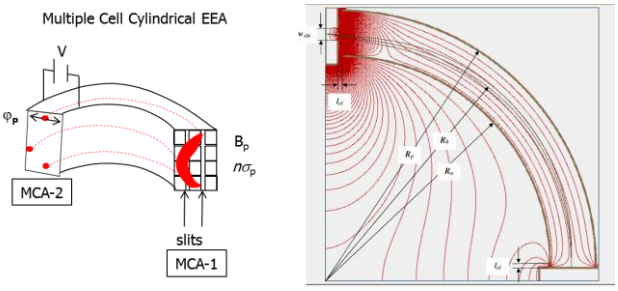

Fig. 13. 90° cylindrical energy analyzer

The best results have been obtained for the initially inclined (θ_{in} = -5°) double charged (q = 2) beam entering the CEA entrance slit slightly below the centerline R_0 (l_{shift} = -2 mm), decelerated from 20 keV to 4 keV passing through the lens formed by fringing field between entrance slit (V_{en} = 0 kV) and CEA plates (V_p = 8.4 kV, V_n = 7.6 kV) and collected on exit electrode kept at V_{ex} = 8 kV. Fig. 14 illustrates visually the energy dispersion (E_0 = 19.7, 20, 20.3 keV, θ_{in} = -5°, Fig. 14,a), focusing (θ_{in} = -7°, -5°, -3°, E_0 = 20 keV, Fig. 14, b) and the magnification (w_{b0} = 2.5 mm, Fig. 14,c) properties of the considered 90° CEA and Gaussian beam.

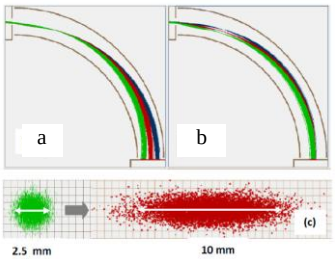

Fig. 14. SIMION results for 90° CEA

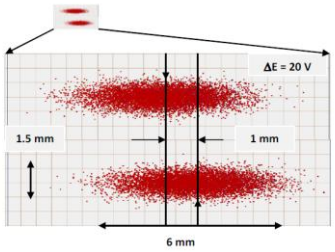

Fig. 15. Resolution property of 90° CEA

Finally, Fig. 15 presents a visual representation of two Gaussian beams w_{b0} =1.5 mm of width and $\Delta\theta = \pm 0.5°$ of divergence differed in energy on 20 V (20 keV top and 20.02 keV bottom). From the figure, the results of numerical simulations of real 90° CEA predicts the energy resolution of $\Delta E/E = 3\times10^{-4}$, that is in the range of plasma potential fluctuations. Also, sufficient decrease of the angular aberration in the range of $\delta\theta = \pm 2°$ is demonstrated. Recalculated to the energy, the residual angle aberration is equivalent to $\Delta E/E = 8.5\times10^{-5}$ of energy change for $\delta\theta = \pm 0.5°$ of expected misalignment and beam divergence ranges.

2.2. REAL-TIME VERTICAL PLASMA POSITION CONTROL

Successful operation of the tokamak relies on the real-time control of plasma position. Such control consists on the measurement, data processing and actuation within an appropriate time window. In the ISTTOK the plasma position is controlled by magnetic fields generated on external coils. The current flowing into the coils is real-time controlled using the ISTTOK control system having a control cycle of 100 μs during which it reads all the plasma position-related diagnostics (Mirnov coils, Langmuir probes) connected to the Advanced Telecommunications Computing Architecture (ATCA) digitizers and sends the control reference to the ISTTOK actuators. The HIBD measures locally and simultaneously the $n_e\sigma_{eff}(T_e)$ product at 12 sample volumes vertically distributed along the plasma region of -0.06 m < r < 0.06 m. Since the plasma equilibrium is related with the plasma pressure and the $n_e\sigma_{eff}(T_e)$ product may be considered as a proxy for the plasma pressure, it is expected that the $n_e\sigma_{eff}(T_e)$ will give more accurate measurements for the plasma position than the currently used diagnostics. A high signal-to-noise ratio of the vertical plasma position measurement is achieved by high, 150 kHz, frequency modulation (chopping) of the primary beam to discriminate the beam signal from the background noise. Providing one profile per chopping period it is

possible to obtain up to 15 $n_e\sigma_{eff}(T_e)$ profiles in one real-time cycle of 100 μs. This work is in the initial stage.

SUMMARY AND FUTURE PLANS

The new MCAD of ISTTOK HIBD is characterized by complete suppression of the plasma background. The improved signal conditioning electronics has high gain, 2×10^7 V/A, low noise <0.5 nA, and high, up to 400 kHz, bandwidth. These improvements allow for detailed study of the plasma MHD activity and the electrode biasing regimes. Except continuation of the work in these areas, the investigations of plasma turbulence and geodesic acoustic mode (GAM) activity are considered in the nearest plans. The implementation of the multichannel multi-slit 90° cylindrical energy analyzer will increase the ISTTOK HIBD performance to measure the plasma potential and its fluctuations. It is important that in simultaneous use of HIBD and LPs, the fluctuations can be measured across the whole plasma cross-section. Also, the work of HIBD use in real-time vertical plasma position control will be continued.

ACKNOWLEDGEMENTS

IPFN activities received financial support from ”Fundação para a Ciência e Tecnologia” through project UID/FIS/50010/2013.

REFERENCES

1. F.C. Jobes, R. L. Hickok // *Nucl. Fusion*. 1970, v. 10, p. 195.
2. J.A.C. Cabral et al. // *Plasma Source Sci. Technol.* 1994, v. 3, p. 1.
3. J.A.C. Cabral, A. Malaquias, A. Praxedes, W. Van Toledo, C.A.F. Varandas // *IEEE Transactions on Plasma Science*. 1994, v. 22(4), p. 350.
4. A. Malaquias, I.S. Nedzelskii, C.A.F. Varandas, J.A.C. Cabral // *Review of Scientific Instruments.* 1999, v. 70(1), p. J947.
5. A. Malaquias, J.A.C. Cabral, C.A.F. Varandas, and R. Canário // *Fusion Engineering and Design*. 1997, v. 34-35, p. 671.
6. R.B. Henriques, I.S. Nedzelskiy, A. Malaquias, H. Fernandes // *Rev. Sci. Instrum.* 2012, v. 83, p. 10D705.
7. R.B. Henriques, A. Malaquias, I.S. Nedzelskiy, C. Silva, R. Coelho, H. Figueiredo, H. Fernandes // *Rev. Sci. Instrum.* 2014, v. 85, p. 11D848.
8. G. Van Oost et al. // *Plasma Phys. Control. Fusion* 2003, v. 45, p. 621.
9. E.P. Benis, T.J.M. Zouros // *Nucl. Instrum. and Meth. in Phys. Res.* Sec. A. 2000, v. 440(2), p. 462.

Article received 19.09.2016

СОВРЕМЕННОЕ СОСТОЯНИЕ ДИАГНОСТИКИ ПЛАЗМЫ ПУЧКА ТЯЖЁЛЫХ ИОНОВ НА ТОКАМАКЕ ISTTOK

И.С. Недзельский, А. Малакиаш, Р.Б. Энрикеш, Р. Шарма

Диагностика пучком тяжёлых ионов (ДПТИ) является мощным инструментом в исследованиях горячей плазмы в термоядерных установках с магнитным удержанием. Инжектируемый в плазму первичный пучок однозарядных положительных ионов ионизируется в двухзарядное состояние в столкновениях с электронами плазмы. В магнитном поле плазменной установки результирующие вторичные ионы отделяются от первичного пучка и детектируются вне плазмы. Измеряемые ДПТИ параметры плазмы включают плотность, температуру электронов, электрический и магнитный потенциалы. На малом токамаке ISTTOK (R = 0,46 м, a = 0,085 м, B = 0,5 Тл, I_p = 4…6 кА, $<n_e> = 5 \times 10^{18}$ м$^{-3}$, T_e = 120 эВ) ДПТИ состоит из 20 кэВ инжектора Xe^+ (или Cs^+) пучка и мультиколлекторного детектора (МКД) вторичных Xe^{2+} (или Cs^{2+}) ионов, выходящих из плазмы вдоль траектории первичного пучка. Описываются изменения и улучшения детекторной системы ДПТИ на токамаке ISTTOK. Возможности новой детекторной системы иллюстрируются недавними результатами исследований МГД-активности и поляризации плазмы. Рассматриваются также разработка многоканального мультищелевого 90° цилиндрического анализатора энергии для измерений потенциала плазмы и его флуктуаций и новый подход использования ДПТИ для контроля вертикального положения плазмы в режиме реального времени.

СУЧАСНИЙ СТАН ДІАГНОСТИКИ ПЛАЗМИ ПУЧКА ВАЖКИХ ІОНІВ НА ТОКАМАЦІ ISTTOK

І.С. Недзельський, А. Малакіаш, Р.Б. Енрікеш, Р. Шарма

Діагностика пучком важких іонів (ДПВІ) є потужним інструментом у дослідженнях гарячої плазми в термоядерних установках з магнітним утриманням. Інжектований в плазму первинний пучок однозарядних позитивних іонів іонізується в двозарядний стан у зіткненнях з електронами плазми. У магнітному полі плазмової установки результуючі вторинні іони відокремлюються від первинного пучка і фіксуються поза плазми. Вимірювані ДПВІ параметри плазми включають щільність, температуру електронів, електричний і магнітний потенціали. На малому токамаці ISTTOK (R = 0,46 м, a = 0,085 м, B = 0,5 Тл, I_p = 4…6 кА, $<n_e> = 5\times10^{18}$ м$^{-3}$, T_e = 120 еВ) ДПВІ складається з 20 кеВ інжектора Xe^+ (або Cs^+) пучка і мультиколекторного детектора (МКД) вторинних Xe^{2+} (або Cs^{2+}) іонів, які виходять з плазми уздовж траєкторії первинного пучка. Описуються зміни і поліпшення детекторної системи ДПВІ на токамаці ISTTOK. Можливості нової детекторної системи ілюструються недавніми результатами досліджень МГД-активності і поляризації плазми. Розглядаються також розробка багатоканального мультищілинного 90° циліндричного аналізатора енергії для вимірювань потенціалу плазми та його флуктуацій і новий підхід використання ДПВІ для контролю вертикального положення плазми в режимі реального часу.